

Understanding the Readiness of Silane Dissociation in Transition Metal η^2 -Silane Complexes $\text{Cp}(\text{CO})_2\text{M}[\eta^2\text{-H}(\text{SiH}_3\text{-}_n\text{Cl}_n)]$ ($\text{M} = \text{Mn, Tc, and Re; } n = 1\text{--}3$)

Sai-Heung Choi, Jianwen Feng, and Zhenyang Lin*

Department of Chemistry, The Hong Kong University of Science and Technology, Clear Water Bay, Kowloon, Hong Kong

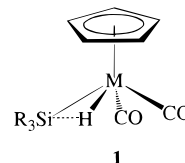
Received November 22, 1999

Summary: The influence of electronegative substituents at silicon and the effect of metal centers on the silane dissociation energies of transition metal η^2 -silane complexes, $\text{Cp}(\text{CO})_2\text{M}[\eta^2\text{-H}(\text{SiH}_3\text{-}_n\text{Cl}_n)]$ ($\text{M} = \text{Mn, Tc, and Re; } n = 1\text{--}3$), were studied by *ab initio* and density functional theory calculations. The $\text{M}\text{--}\text{Si}$ and $\text{Si}\cdots\text{H}$ interactions in relation to the readiness of silane dissociation are also examined. The calculated dissociation energies are found to increase down the group as a result of the more diffuse *d* orbitals for the third-series transition metal. The dissociation energies also increase with the number of the chloride substituents. With the increase of the chloride substituents, the $\text{M}\text{--}\text{Si}$ interaction is significantly enhanced and is responsible for the increasing dissociation energies. The $\text{Si}\cdots\text{H}$ distances do not decrease as a result of increasing $\text{M}\text{--}\text{Si}$ interaction when the chloride substituents at silicon increase. These results are related to the tendency of the silicon center to be hypervalent.

Introduction

Transition metal η^2 -silane complexes have gained immense research interest in synthetic, structural, and theoretical aspects over the past two decades,¹ as they are important intermediates in metal-catalyzed hydrosilylation reactions^{11,2} and models for C–H activation.³ Complexes with group 7 metals, $\text{Cp}(\text{CO})_2\text{M}(\eta^2\text{-HSiR}_3)$ **1**, are prototypical examples that can be isolated by oxidative addition reaction of silanes, HSiR_3 to $\text{Cp}(\text{CO})_2\text{M}$.^{1a,4} However, a complete oxidative addition will result in a total cleavage of the Si–H bond and lead to

the formation of hydridosilane, $\text{Cp}(\text{CO})_2\text{M}(\text{H})(\text{SiR}_3)$. This oxidative addition reaction may be reversible because of the facile dissociation of silane from its parent complex.¹¹



The reverse reductive elimination reaction, namely, silane dissociation of **1**, has been thoroughly investigated.^{4–9} Detailed studies of the silane dissociation processes showed that the readiness of silane dissociation is associated with both the electron-richness of the metal center and the electronic properties of substituents at silicon. It was found that silane dissociates more slowly for complexes with electron-rich metal centers or more electronegative substituents at silicon.^{11,4,10,11} For example, $\text{Cp}(\text{CO})_2\text{Re}(\eta^2\text{-HSiPh}_3)$ undergoes silane dissociation much slower than the corresponding manganese complex, $\text{Cp}(\text{CO})_2\text{Mn}(\eta^2\text{-HSiPh}_3)$.⁵ Also, HSiCl_3 is eliminated 10^5 times more slowly from $\text{Cp}(\text{CO})_2\text{Mn}(\eta^2\text{-HSiCl}_3)$ than HSiPh_3 from $\text{Cp}(\text{CO})_2\text{Mn}(\eta^2\text{-HSiPh}_3)$ at 100°C .⁴ It is a common belief that for a $\text{L}_m\text{M}(\eta^2\text{-H-X})$ complex, the dissociation of H–X can be facilitated if the H–X interaction in the parent complex remains strong. From the experimental observations, it was therefore inferred that the $\text{Si}\cdots\text{H}$ distance (see **1** for structural information) is shorter in $\text{Cp}(\text{CO})_2\text{Mn}(\eta^2\text{-HSiPh}_3)$ than that in $\text{Cp}(\text{CO})_2\text{Mn}(\eta^2\text{-HSiCl}_3)$.¹⁰

In contrast, the previous theoretical studies¹² on the family of $\text{Cp}_2\text{MXH}(\text{SiCl}_n\text{H}_{3-n})$ ($\text{M} = \text{Nb and Ta; X} = \text{SiH}_3, \text{Cl, H, and CH}_3; n = 0\text{--}3$) at both the MP2 and B3LYP levels have demonstrated that stronger $\text{Si}\cdots\text{H}$

(1) (a) Graham, W. A. G. *J. Organomet. Chem.* **1986**, *300*, 81. (b) Raba , H.; Saillard, J.-Y.; Schubert, U. *J. Organomet. Chem.* **1987**, *330*, 397. (c) Schubert, U. *Adv. Organomet. Chem.* **1990**, *30*, 151. (d) Schubert, U. *Transition Met. Chem.* **1991**, *16*, 136. (e) Crabtree, R. H. *Angew. Chem., Int. Ed. Engl.* **1993**, *32*, 789. (f) Luo, X.-L.; Kubas, G. J.; Burns, C. J.; Bryan, J. C.; Unkefer, C. J. *J. Am. Chem. Soc.* **1995**, *117*, 1159. (g) Schneider, J. *Angew. Chem., Int. Ed. Engl.* **1996**, *35*, 1068. (h) Peulecke, N.; Ohff, A.; Kosse, P.; Tillack, A.; Spannenberg, A.; Kempe, R.; Baumann, W.; Burlakov, V. V.; Rosenthal, U. *Chem. Eur. J.* **1998**, *4*, 1852. (i) Corey, J. Y.; Braddock-Wilking, J. *Chem. Rev.* **1999**, *99*, 175. (j) Delpech, F.; Sabo-Etienne, S.; Daran, J.; Chaudret, B.; Hussein, K.; Marsden, C. J.; Barthelat, J. *J. Am. Chem. Soc.* **1999**, *121*, 6668.

(2) (a) Speier, J. L. *Adv. Organomet. Chem.* **1977**, *17*, 407. (b) Parshall, G. W. *Homogeneous Catalysis: the Application and Chemistry of Catalysis by Soluble Transition Metal Complexes*; Wiley: New York, 1992; p 39.

(3) (a) *Selective Hydrocarbon Activation: Principles and Progress*; Davies, J. A., Ed.; VCH Publishers: New York, 1990. (b) Pines, H. *The Chemistry of Catalytic Hydrocarbon Conversions*; Academic Press: New York, 1981. (c) Crabtree, R. H. *Chem. Rev.* **1995**, *95*, 987. (d) Schneider, J. *Angew. Chem., Int. Ed. Engl.* **1996**, *35*, 1068.

(4) Hart-Davis, A. J.; Graham, W. A. G. *J. Am. Chem. Soc.* **1971**, *93*, 4388.

(5) Dong, D. F.; Hoyano, J. K.; Graham, A. G. *Can. J. of Chem.* **1981**, *59*, 1455.

(6) Colomer, E.; Corriu, R. J. P.; Vioux, A. *Inorg. Chem.* **1979**, *18*, 695.

(7) Schubert, U.; Scholz, G.; M ller, J.; Ackermann, K.; W rle, B. *J. Organomet. Chem.* **1986**, *306*, 303.

(8) Lichtenberger, D. L.; Rai-Chaudhuri, A. *J. Am. Chem. Soc.* **1989**, *111*, 3583.

(9) (a) Yang, H.; Kotz, K. T.; Asplund, M. C.; Harris, C. B. *J. Am. Chem. Soc.* **1997**, *119*, 9564. (b) Yang, H.; Asplund, M. C.; Kotz, K. T.; Wilkens, M. J.; Frei, H.; Harris, C. B. *J. Am. Chem. Soc.* **1998**, *120*, 10154.

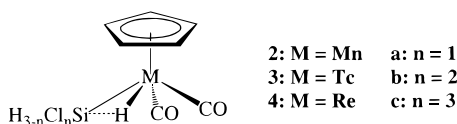
(10) Schubert, U.; Ackermann, K.; W rle, B. *J. Am. Chem. Soc.* **1982**, *104*, 7378.

(11) Carr , F.; Colomer, E.; Corriu, R. J. P.; Vioux, A. *Organometallics* **1984**, *3*, 1272.

(12) Fan, M.-F.; Lin, Z. *Organometallics* **1998**, *17*, 1092.

interaction is observed for complexes that have more chloride substituents at silicon. The increasing Si...H interaction is related to the hypervalency of the silicon center.^{12,13} Here, "hypervalent" refers to the expansion of octet surrounding the Si center.

These two different conclusions regarding the influence on Si...H interaction by substituents on the silicon moiety have prompted us to undergo a systematic theoretical study on the nature of transition metal-(η^2 -silane) interaction and to investigate the readiness of silane dissociation in a series of complexes $\text{Cp}(\text{CO})_2\text{M}[\eta^2\text{-H}(\text{SiCl}_n\text{H}_{3-n})]$ ($\text{M} = \text{Mn, Tc, and Re}$; $n = 1-3$). Through the calculations of structures and silane dissociation energies for these complexes, we attempt to provide computational evidence to clarify these experimental and theoretical observations mentioned above.



Computational Details

Model complexes $\text{Cp}(\text{CO})_2\text{M}[\eta^2\text{-H}(\text{SiCl}_n\text{H}_{3-n})]$ ($n = 1-3$), **2**, **3**, and **4** with different metal centers ($\text{M} = \text{Mn, Tc, and Re}$) were used to study the influence of metal centers on the readiness of silane dissociation. To mimic various electronic environments around the Si center, successive increase of the Cl substitutions ($n = 1-3$) at Si is applied to each model. The descriptors **a-c** denote complexes with the silane ligand containing 1-3 chloride substituents.

Geometry optimizations were performed at both the second-order Møller-Plesset perturbation theory¹⁴ (MP2) and Becke-3LYP¹⁵ (B3LYP) levels. These two levels of calculations have been shown to reproduce experimental structural parameters well for several types of nonclassical transition metal complexes including transition metal η^2 -silane and dihydrogen complexes.^{12,13,16} The standard 6-31G basis set¹⁷ was used for elements of the first and second periods, while effective core potentials (ECPs) of Hay and Wadt with double- ξ valence basis set (LanL2DZ)¹⁸ were used to describe other heavy elements. The hydrogen and silicon atoms involved in the η^2 -silane moiety were augmented with polarization functions, namely, p-polarization functions (i.e., 6-31G**) for H and d-polarization functions of Huzinaga¹⁹ ($\xi = 0.282$) for Si. In addition to the dissociation energies calculated at the MP2 and B3LYP levels, single-point CISD²⁰ calculations based on the optimized structures at both levels were also performed. For these single-point CISD calculations, the active spaces being chosen do not

Table 1. Selected Bond Lengths (Å) that Involve the $\text{M}\cdots(\eta^2\text{-HSi})$ Interaction of Model Complexes **2, **3**, and **4** for $n = 1-3$ at the MP2 and B3LYP Levels**

		MP2			B3LYP		
		a ($n = 1$)	b ($n = 2$)	c ($n = 3$)	a ($n = 1$)	b ($n = 2$)	c ($n = 3$)
2	Mn-Si	2.297	2.255	2.216	2.369	2.328	2.302
	Mn-H	1.457	1.463	1.469	1.550	1.544	1.545
	Si...H	1.841	1.815	1.806	1.728	1.734	1.732
3	Tc-Si	2.440	2.403	2.375	2.475	2.443	2.420
	Tc-H	1.643	1.642	1.642	1.671	1.669	1.666
	Si...H	1.969	1.960	1.935	1.879	1.882	1.881
4	Re-Si	2.450	2.415	2.389	2.480	2.451	2.431
	Re-H	1.654	1.651	1.650	1.673	1.671	1.668
	Si...H	2.043	2.036	2.018	2.011	2.018	2.028

include core orbitals, the σ -bonding orbitals of the Cp and CO ligands, and the lone pairs of O and Cl atoms. To further reduce the computational cost, virtual orbitals higher than 5.00 au in their orbital energies are also excluded from the active space.

One of the reviewers was concerned about the LanL2DZ basis set adequately representing the transition metal bonding. We optimize **2c** at the B3LYP level with the Stuttgart/Dresden ECP (SDD) basis set,²¹ which augments diffuse functions for valence orbitals, for the heavy elements. The calculation with this larger basis set gives almost no change in the structural parameters when compared to the those from the corresponding LanL2DZ results. The changes in bond lengths and angles are within 0.04 Å and 1°, respectively. The silane dissociation energy was calculated to be 29.23 kcal/mol, only slightly greater than the corresponding LanL2DZ result (27.69 kcal/mol). All the calculations were performed with the Gaussian98 software package²² on a Silicon Graphics Indigo² workstation.

Results and Discussion

$\text{M}\cdots(\eta^2\text{-HSi})$ Interaction in $\text{Cp}(\text{CO})_2\text{M}[\eta^2\text{-H}(\text{SiH}_{3-n}\text{Cl}_n)]$ Complexes. Structural parameters involving the $\text{M}\cdots(\eta^2\text{-HSi})$ interaction of the optimized structures of models **2**, **3**, and **4** for various chloride substitutions ($n = 1-3$) are summarized in Table 1. Among these model complexes, the theoretically determined bond lengths involving the $\text{M}\cdots(\eta^2\text{-HSi})$ interaction in **2c**, $\text{Cp}(\text{CO})_2\text{Mn}(\eta^2\text{-HSiCl}_3)$, and those of the experimentally observed complex $\text{MeCp}(\text{CO})_2\text{Mn}(\eta^2\text{-HSiCl}_3)$, as determined by X-ray crystallography, are in good agreement at both levels (Figure 1a). To further assess the accuracy of theoretical levels used in our calculations, geometry optimization was done for $\text{Cp}(\text{CO})_2\text{Mn}(\eta^2\text{-HSiFH}_2)$. Comparison is also made with the

(13) (a) Nikonov, G. I.; Kuzmina, L. G.; Lemenovskii, D. A.; Kotov, V. V. *J. Am. Chem. Soc.* **1995**, *117*, 10133. (b) Nikonov, G. I.; Kuzmina, L. G.; Lemenovskii, D. A.; Kotov, V. V. *J. Am. Chem. Soc.* **1996**, *118*, 6333. (c) Nikonov, G. I.; Kuzmina, L. G.; Vyboishchikov, S. F.; Lemenovskii, D. A.; Howard, J. A. K. *Chem. Eur. J.* **1999**, *5*, 2917.

(14) (a) Head-Gordon, M.; Pople, J. A.; Frisch, M. J. *Chem. Phys. Lett.* **1988**, *153*, 503. (b) Saebø, S.; Almlof, J. *Chem. Phys. Lett.* **1989**, *154*, 83. (c) Frisch, M. J.; Head-Gordon, M.; Pople, J. A. *Chem. Phys. Lett.* **1990**, *166*, 275. (d) Frisch, M. J.; Head-Gordon, M.; Pople, J. A. *Chem. Phys. Lett.* **1990**, *166*, 281.

(15) (a) Becke, A. D. *J. Chem. Phys.* **1993**, *98*, 5648. (b) Miehlich, B.; Savin, A.; Stoll, H.; Preuss, H. *Chem. Phys. Lett.* **1989**, *157*, 200. (c) Lee, C.; Yang, W.; Parr, G. *Phys. Rev. B* **1988**, *37*, 785.

(16) (a) Fan, M.-F.; Lin, Z. *Organometallics* **1999**, *18*, 286. (b) Fan, M.-F.; Lin, Z. *Organometallics* **1997**, *16*, 494. (c) Fan, M.-F.; Jia, G.; Lin, Z. *J. Am. Chem. Soc.* **1996**, *118*, 9915. (d) Maseras, F.; Lledos, A.; Costas, M.; Poblet, J. M. *Organometallics* **1996**, *15*, 2947.

(17) Hariharan, P. C.; Pople, J. A. *Theor. Chim. Acta* **1973**, *28*, 213.

(18) (a) Hay, P. J.; Wadt, W. R. *J. Chem. Phys.* **1985**, *82*, 270. (b) Wadt, W. R.; Hay, P. J. *J. Chem. Phys.* **1985**, *82*, 284. (c) Hay, P. J.; Wadt, W. R. *J. Chem. Phys.* **1985**, *82*, 299.

(19) Andzelm, J.; Huzinaga, S. *Gaussian Basis Sets for Molecular Calculations*; Elsevier: New York, 1984.

(20) (a) Krishnan, R.; Schlegel, H. B.; Pople, J. A. *J. Chem. Phys.* **1980**, *72*, 4654. (b) Raghavachari, K.; Pople, J. A. *Int. J. Quantum Chem.* **1981**, *20*, 167.

(21) (a) Haeussermann, U.; Dolg, M.; Stoll, H.; Preuss, H. *Mol. Phys.* **1993**, *78*, 1211. (b) Kuechle, W.; Dolg, M.; Stoll, H.; Preuss, H. *J. Chem. Phys.* **1994**, *100*, 7535. (c) Nicklass, A.; Dolg, M.; Stoll, H.; Preuss, H. *J. Chem. Phys.* **1995**, *102*, 8942. (d) Leininger, T.; Nicklass, A.; Stoll, H.; Dolg, M.; Schwerdtfeger, P. *J. Chem. Phys.* **1996**, *105*, 1052.

(22) Frisch, M. J.; Trucks, G. W.; Schlegel, H. B.; Scuseria, G. E.; Robb, M. A.; Cheeseman, J. R.; Zakrzewski, V. G.; Montgomery, J. A., Jr.; Stratmann, R. E.; Burant, J. C.; Dapprich, S.; Millam, J. M.; Daniels, A. D.; Kudin, K. N.; Strain, M. C.; Farkas, O.; Tomasi, J.; Barone, V.; Cossi, M.; Cammi, R.; Mennucci, B.; Pomelli, C.; Adamo, C.; Clifford, S.; Ochterski, J.; Petersson, G. A.; Ayala, P. Y.; Cui, Q.; Morokuma, K.; Malick, D. K.; Rabuck, A. D.; Raghavachari, K.; Foresman, J. B.; Cioslowski, J.; Ortiz, J. V.; Stefanov, B. B.; Liu, G.; Liashenko, A.; Piskorz, P.; Komaromi, I.; Gomperts, R.; Martin, R. L.; Fox, D. J.; Keith, T.; Al-Laham, M. A.; Peng, C. Y.; Nanayakkara, A.; Gonzalez, C.; Challacombe, M.; Gill, P. M. W.; Johnson, B.; Chen, W.; Wong, M. W.; Andres, J. L.; Gonzalez, C.; Head-Gordon, M.; Replogle, E. S.; Pople, J. A. *Gaussian 98 (Revision A.5)*; Gaussian, Inc.: Pittsburgh, PA, 1998.

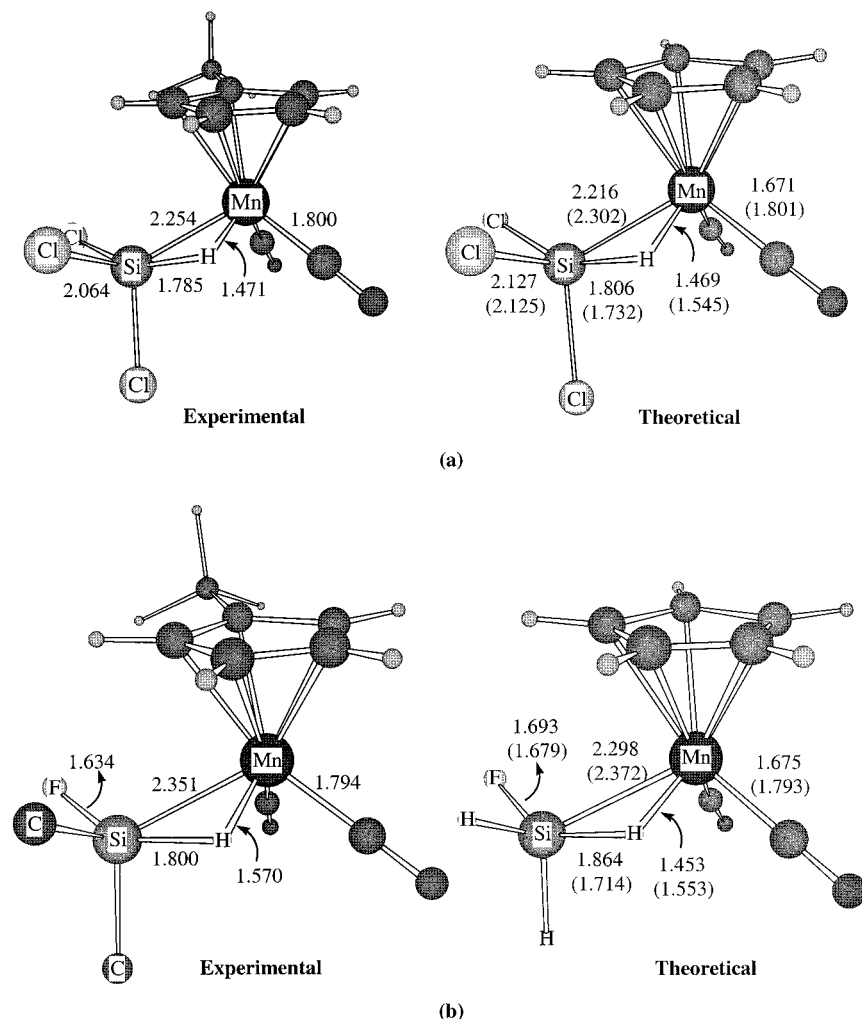


Figure 1. Comparison between experimental and MP2 (B3LYP) calculated geometries. (a) The X-ray determined complex $\text{MeCp}(\text{CO})_2\text{Mn}(\eta^2\text{-HSiCl}_3)$ and model complex $\text{Cp}(\text{CO})_2\text{Mn}(\eta^2\text{-HSiCl}_3)$, **2c**. (b) The neutron diffraction determined complex $\text{MeCp}(\text{CO})_2\text{Mn}(\eta^2\text{-HSiFPh}_2)$ and model complex $\text{Cp}(\text{CO})_2\text{Mn}(\eta^2\text{-HSiFH}_2)$. For the experimental complexes, each phenyl group on Si is substituted by one atom for clarity.

neutron diffraction determined complex $\text{MeCp}(\text{CO})_2\text{Mn}(\eta^2\text{-HSiFPh}_2)$ (Figure 1b). The agreement between the calculated and experimental geometries is also good.

For a given metal, Table 1 clearly shows that successive substitution of H atoms by Cl atoms at silicon results in a considerable decrease in the M–Si distances, greater than 0.05 Å (the change in M–Si from $n = 1$ to 3), whereas the M–H distances almost remain constant upon substitution for all models at both levels. In contrast, the Si···H distances decrease only moderately from $n = 1$ to $n = 3$ at the MP2 level and show little change at the B3LYP level. We can see that the overall changes in the Si···H distances are much less significant when compared to the changes observed for the M–Si distances. These results are in good agreement with the experimental observation in which the Si···H distances do not change much upon substitution of electronegative substituents at silicon.¹¹ For example, the reported Si···H distances of $\text{Cp}(\text{CO})_2\text{Mn}(\eta^2\text{-HSiPh}_3)$ and $\text{Cp}(\text{CO})_2\text{Mn}(\eta^2\text{-HSiCl}_2\text{Ph})$ are 1.76 and 1.79 Å, respectively.^{1c}

To make a comparison of the Si···H distances between models with different metal centers, we found that the corresponding Si···H distances increase significantly from M = Mn to Tc, and then to Re. Indeed, the long

Si···H distances in the Re complexes, **4a–c**, which are greater than 2.0 Å, indicate that these transition metal complexes are more classical. Experimentally, the X-ray determined Si···H distance of $\text{Cp}(\text{CO})_2\text{Re}(\eta^2\text{-HSiPh}_3)$ is 2.19 Å.^{2a} The increasing Si···H distance down the group is related to their greater reducing ability and more diffuse d orbitals of higher period transition metals. It is also worthy to note that the M–Si distances increase down the group. The M–Si distances increase more significantly from the first-row transition metal complexes to the second-row complexes. This trend is consistent with the changes in the radii of the transition metal atoms that increase down the group, especially between the first two rows.

Dissociation Energies of $\text{Cp}(\text{CO})_2\text{M}[\eta^2\text{-H}(\text{SiH}_{3-n}\text{Cl}_n)]$ Complexes. The dissociation energies of model complexes **2**, **3**, and **4** calculated at the MP2, B3LYP, CISD//MP2, and CISD//B3LYP levels, as defined by $\text{DE} = E\{\text{Cp}(\text{CO})_2\text{M}[\eta^2\text{-H}(\text{SiH}_{3-n}\text{Cl}_n)]\} - \{E[\text{Cp}(\text{CO})_2\text{M}] + E[\text{SiH}_{3-n}\text{Cl}_n]\}$,²³ are listed in Table 2. It is found that the calculated dissociation energies at the MP2 level differ greatly from those at the B3LYP level (see values in parentheses in Table 2). However, the results from the CISD//MP2 and CISD//B3LYP calculations are reasonably consistent for the Tc and Re

Table 2. Calculated Silane Dissociation Energies (kcal/mol) of Model Complexes 2, 3, and 4 for $n = 1-3$ at the CISD Level^a

	CISD//MP2			CISD//B3LYP		
	a ($n = 1$)	b ($n = 2$)	c ($n = 3$)	a ($n = 1$)	b ($n = 2$)	c ($n = 3$)
2 (Mn)	5.34 (73.78)	9.74 (77.22)	12.87 (83.13)	20.63 (21.90)	24.34 (23.98)	27.63 (27.69)
3 (Tc)	36.78 (59.71)	40.75 (64.97)	43.73 (68.74)	36.74 (30.58)	40.73 (33.52)	43.79 (36.08)
4 (Re)	51.36 (70.06)	55.72 (75.39)	58.52 (79.18)	51.40 (43.16)	55.80 (46.33)	58.72 (48.86)

^a The corresponding dissociation energies (kcal/mol) predetermined at the MP2 and B3LYP levels are given in parenthesis.

complexes. From Table 2, it also can be seen that the B3LYP dissociation energies do not differ much from the CISD dissociation energies. These results are consistent with the claim that dissociation energies determined at the B3LYP level are more reasonable, and MP2 calculations tend to significantly overestimate dissociation energies.²⁴ The optimized geometries for the Tc and Re complexes at the MP2 level do not differ much from those obtained at the B3LYP level. Therefore, the CISD//MP2 and CISD//B3LYP levels of theory give consistent results for both the Tc and Re complexes.

However, for the Mn complexes the optimized geometries at MP2 and B3LYP differ significantly in the Mn(CO)₂ moiety. The MP2 calculations severely underestimate the Mn–CO distances. For example, the experimental observed Mn–CO distance in Cp(CO)₂Mn(η^2 -HSiCl₃) is 1.785 Å, whereas the MP2 calculation gives only 1.671 Å (see Figure 1a). The poorly optimized geometries obtained at the MP2 level for the Mn complexes result in the significant underestimation of dissociation energies at the CISD//MP2 level.

To further understand the discrepancy between the MP2 and B3LYP results, calculations at the MP2//B3LYP and B3LYP//MP2 levels were performed for Cp(CO)₂Mn(η^2 -HSiCl₃). The dissociation energy calculated at MP2//B3LYP is 68.69 kcal/mol, significantly greater than the CISD calculations. This result reveals that the overestimation of dissociation energies is inherent at the MP2 level. The dissociation energy calculated at B3LYP//MP2 (13.67 kcal/mol) is close to that calculated at the CISD//MP2 level (12.87 kcal/mol). This result suggests that the geometries obtained at the MP2 level, which inadequately reproduces the Mn–CO interactions, give much smaller dissociation energies.

Chemically more important are the trends observed from these calculations. Table 2 clearly shows that for a given metal dissociation energies increase as the number of Cl substituents at silicon increases. This

trend is consistent with the experimental observations that HSiCl₃ dissociates much slower from Cp(CO)₂Mn(η^2 -HSiCl₃) when compared to the dissociation of HSiPh₃ from Cp(CO)₂Mn(η^2 -HSiPh₃).⁴ When going down the group, calculation results indicate that dissociation energies also increase. Among these model complexes, the Re complexes, **4a–c**, give the greatest dissociation energies. These results are in good agreement with the experimental observation for which Cp(CO)₂Re(η^2 -HSiPh₃) undergoes a silane dissociation much slower than for the corresponding manganese complex.⁵ The more diffuse d orbitals of higher period transition metals are apparently responsible for the observed trend. The same trend was also observed for the first carbonyl dissociation of the group 6 M(CO)₆ complexes.²⁵

Summary. In this note, silane dissociations of Cp(CO)₂M[η^2 -H(SiH_{3– n Cl _{n})] complexes for M = Mn, Tc, and Re; $n = 1-3$, were investigated theoretically. The variation of the M \cdots (η^2 -HSi) interactions in these complexes upon Cl substitutions and the effect of the metal center were also studied. For a given metal center, the silane dissociation energies increase with the increase of the Cl substituents. Structurally, we observed that with the increase of the Cl substituents the M–Si distances are significantly shortened while the M–H distances remain approximately unchanged. The Si \cdots H distances, however, do not change significantly. At the MP2 level, the distances slightly decrease, while the B3LYP results show little change. These results suggest that the increase of the dissociation energy with the increase of Cl substituents is a result of increasing M–Si interaction. Contrary to the common belief, the M–Si interaction does not increase at the expense of weakening the Si \cdots H interaction. This suggests that the behavior of Si is rather different when compared to other second-row main group atoms. In other L _{n} M(η^2 -H–X) complexes when the H-bonded atom in the X group is a second-row element, it is expected that the stronger the M–X interaction, the weaker the H \cdots X interaction. However, due to the tendency of the silicon center to be hypervalent, the commonly accepted viewpoint is not necessarily applicable. The silane dissociation energies increase down the group because of more diffuse d orbitals for a heavier metal. The Si \cdots H distances increase as well, following the normal trend as expected. These results are in accord with the notion that the substitution of more electronegative ligands at silicon plays a more significant role toward the hypervalency of silicon.}

Acknowledgment. This work was supported by the Research Grants Council of Hong Kong and the Hong Kong University of Science and Technology.

OM990920U

(23) Maseras, F.; Lledós, A. *Organometallics* **1996**, *15*, 1218.

(24) (a) Dapprich, S.; Frenking, G. *Organometallics* **1996**, *15*, 4547.
(b) Frenking, G.; Antes, I.; Bohme, M. *Reviews in Computational Chemistry*; Lipkowitz, K. B., Boyd, D. B., Eds.; VCH: New York, 1996; Vol. VIII, pp 63–144.

(25) Ehlers, A. W.; Frenking, G. *J. Am. Chem. Soc.* **1994**, *116*, 1514.